Effect of the Residual Porosity of CoCrMo Bearing Parts Produced by Additive Manufacturing on Wear of Polyethylene

Augustin Lerebours, Clémence Demangel, Lucas Dembinski, Salima Bouvier, Alain Rassineux, Christophe Egles

Effect of the residual porosity of CoCrMo bearing parts produced by additive manufacturing on wear of polyethylene

Augustin LEREBOURS[1*], Clémence DEMANGEL[2], Lucas DEMBINSKI[3], Salima BOUVIER[1], Alain RASSINEUX[1], Christophe EGLES[4].

[1] Alliance Sorbonne Université, Université de technologie de Compiègne, CNRS, FRE 2012 Roberval, Centre de recherche Royallieu, CS 60 319, 60 203 Compiègne cedex, France ; augustin.lerebours@utc.fr, salima.bouvier@utc.fr, alain.rassineux@utc.fr

[2] CRITT-MDTS, 3 bd Jean Delautre F-08000 Charleville-Mézières, France, c.demangel@critt-mdts.com

[3] LERMPS, ICB UMR 6303, CNRS, Univ. Bourgogne Franche-Comté, UTBM, F-90010 Belfort, France

[4] Alliance Sorbonne Université, Université de technologie de Compiègne, CNRS, UMR 7338 BioMécanique et BioIngénierie (BMBI), Centre de recherche Royallieu, CS 60 319, 60 203 Compiègne cedex, France ; christophe.egles@utc.fr.

***Corresponding author :** Augustin LEREBOURS, Alliance Sorbonne Université, Université de technologie de Compiègne, CNRS, FRE-2012 Roberval, Centre de recherche Royallieu, CS 60 319, 60 203 Compiègne cedex, France ; phone number: +33 6 58 01 99 46, Email : augustin.lerebours@utc.fr,

Abstract

Additive manufacturing (AM) has proven to be a flexible technique to create complex designs layer-by-layer. Among others, this versatility has disabled the production of advanced total joint replacements. The high degree of customization offered by AM provides countless opportunities to empower the fabrication accuracy of complex biomaterial constructs to tailor patient-specific implants according to their morphology and pathology. In addition, AM offers interesting microarchitecture control of surfaces, which influences biotribological performances. Porosity is an inherent defect of AM-based metallic material and has been shown to affect mechanical performances such as tensile stress. Thus, in the context of bearing surfaces of artificial joints, this article aims to understand the physical behavior of AM-created cavities on the wear performance of polyethylene in a synovial-like environment with a multidirectional pin-on-disc machine at 37°C.

The article provides quantitative ultra-high molecular weight polyethylene wear results against AM-based cobalt-based alloy parts with a gradient of cavities. The results demonstrate a strong correlation between mass loss of UHMWPE and the total surface porosity defects in the metallic counterparts. Reducing the surface porosity of AM parts is therefore beneficial for improving the wear resistance of UHMWPE.

This work not only underlines the negative effect of metallic surface cavities in the wear resistance of UHMWPE but also gives some understanding of the physical behavior of metallic cavities produced by AM. The AM-created cavities modify adhesion wear and abrasion wear mechanisms. Interestingly the pores also limit the abrasive effect of a third body particles by acting as debris collector.

Keywords

Additive manufacturing, Selective laser melting, Polyethylene wear, Cobalt-chromium-molybdenum alloy, Porosity, Total joint replacement.

Abbreviations

AM, additive manufacturing; SLM, selective laser melting; 3D, three-Dimensional; CoCrMo, Cobalt-chromium-molybdenum alloy; UHMWPE, ultra high molecular weight polyethylene; SEM, Scanning Electron, EBSD, Electron backscatter diffraction.

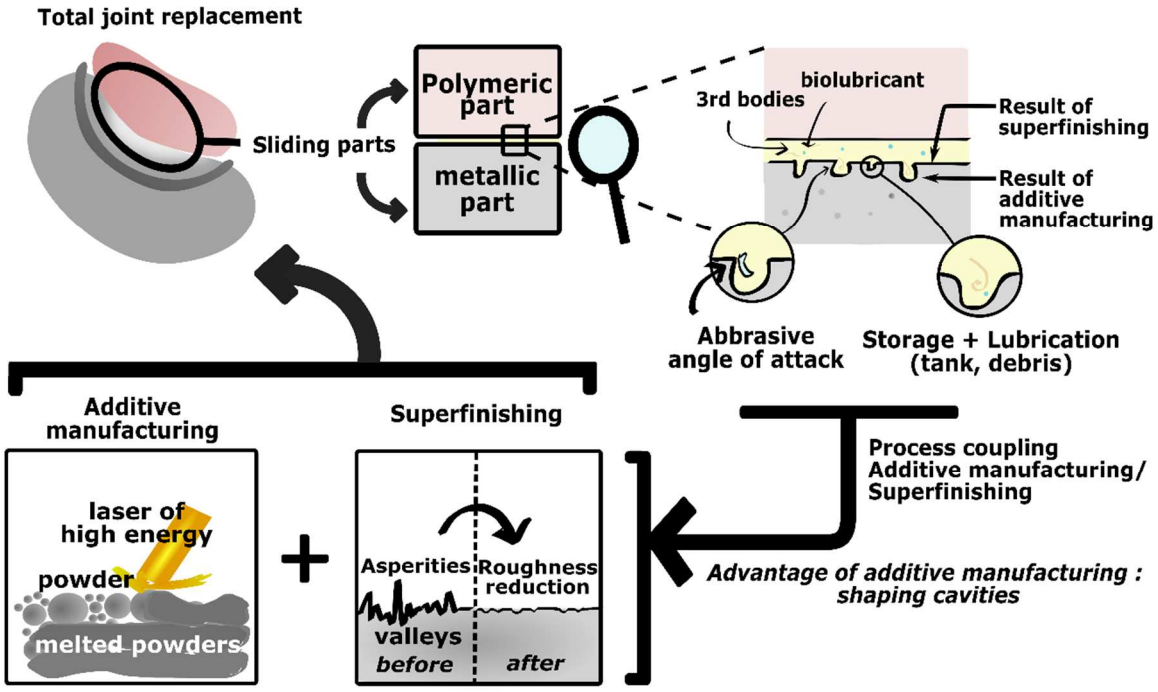

Graphical abstract

1 Introduction

Additive manufacturing (AM) allows the creation of parts with complex internal and external geometry by adding material layer by layer directly from computer-assisted-design (CAD) according to ASTM standard F2792-10 and ISO 17296. AM enabled customized manufacturing of implants matching patient's anatomy which may be further adapted to the stage attained by the pathology [1,2]. Compared to traditionally manufactured implants with standard dimensions, AM creates unique and accurate implants for various orthopedic and traumatological purposes such as knee arthroplasty, spinal deformities and dental replacement [3]. Accurately fitting total joint replacement implants along with specific surgical guides help the surgeon complete the surgical implantation precisely and successfully within a shorter operative time [4]. In fact, demand for patient-specific bone and joint implants has become inherent in order to palliate osteoporosis, arthritis and traumatic musculoskeletal injuries [5].

Among AM technologies, production of metal parts through Selective Laser Melting (SLM) has been possible thanks to high-power laser which progressively and locally fuses metal powder in a controlled atmosphere (Ar, N_2, H_2).

The manufacturing process is complex as it possesses many parameters which all play a role in producing fully dense parts with minimum internal stress. These parameters include (i) the laser parameters (power, scanning speed, beam diameter, etc), (ii) the system parameters (thickness of the powder layer, the treated powder surface, hatch space, the scanning strategies, etc), (iii) the environmental parameters (preheating temperature, the atmosphere and gas pressures) and (iv) the powders characteristics (morphology, size, distribution) [6]. Metal additive manufacturing offers many advantages: (i) freedom of design in relation to subtractive processes, (ii) lighter structures possible either by lattice structures or by the design of parts where the material is only where it is needed without further constraints, (iii) new functions such as complex internal channels, (iv) net shape process leading to less raw material consumption and reducing the number of assembly operations and tools needed, (v) short production cycle time for complex parts.

SLM creates unique material characteristics which thereby might modify the mechanical, biological and physico-chemical properties. The process consists of melting and solidifying a small surface of metallic powders with a laser beam of high energy. The thermal history due to the rapid melting and solidification of the material leads to fine microstructural properties. Most of the materials made by SLM are found to be anisotropic. An anisotropy in the Z direction is due to the superposition of layers while an anisotropy in X-Y directions is related to the scanning strategy (scan vector lengths and scan vector rotation) [7,8]. Typical defects can be observed including partially melted particles, lack of fusion, pores, cracks and inclusions [7]. Such defects can be linked to poor process parameters optimization, construction strategy, part orientation or inadequate powder quality.

Pores in the parts created by SLM can significantly affect their mechanical behavior and therefore their performance [9,10]. Thus, in many applications, the objective is to obtain full dense parts without any porosity. Parameters optimization may be a challenge for some materials that poorly accommodate high internal stress during the fabrication process [11]. Finely tuned manufacturing parameters coupled with specific post-treatments (e.g. hot isostatic pressing) allows a reduction of the porosity but not its complete disappearance. The presence of open pores to the surface are particularly difficult to remove [12,13]. Thus, in the context of bearing surfaces of artificial joints, this article aims to understand the physical behavior of AM-based cavities on the wear performance of polyethylene in a synovial-like environment.

Metal additive manufacturing especially SLM has enabled the production of cobalt-chromium-molybdenum (CoCrMo) parts with complex geometries [14,15]. CoCrMo alloy is a biocompatible material which has been widely used for orthopedic implant [16,17] along with ultra high molecular weight polyethylene (UHMWPE). This material combination is common for articular implants such as knee and hip replacement implants [18] and therefore was selected for this work. The cobalt based alloy was produced by selective laser melting and UHMWPE was molded (ASTM F72, ISO 5834-2).

Our study focuses on the polyethylene mass loss under metallic surfaces that have a gradient of porosity defect under lubricated conditions in order to control the performance of the parts for further artificial joint implant applications. Joint fluid was simulated by diluted bovine serum.

This work is particularly important regarding the development of complex geometric AM-based implant.

Firstly, we tackled the production feasibility of selective laser melted CoCrMo parts with a surface texture in accordance with the specifications of ISO 21534:2007 standard. Secondly, in order to meet application requirements, we used a superfinishing process which can also be applied to complex geometric parts.

This is the first report to study the biotribological physical behavior of the cavities produced by metal-AM on the UHMWPE wear.

2 Material and methods

2.1 Specimens

Cylindrical discs of a 10mm radius and 5mm thickness were manufactured by SLM in CoCrMo. The control material was a cast-CoCrMo. UHMWPE pins were machined from an extruded UHMWPE bar GUR 1020 (chirulen®, Quadrant™) [19]. The polyethylene bar was thermally stabilized under inert atmosphere and was not irradiated. Pins comprise respectively a radius and a length of 3.5mm and 30mm.

The manufacturing process of the CoCrMo discs includes (i) SLM of the disc from CoCrMo powder, (ii) removal of the SLM supports, (iii) cleaning of the specimens by a sandblasting process (iv) superfinishing of the specimens by micromachining process and (v) removal of the micromachining supports.

Three different types of CoCrMo-discs were produced with gradual porosity defects in order to understand their impact on the wear behavior of UHMWPE. Surface texture and cavity characteristics are subsequently described in the results and discussion section.

2.1.1 CoCrMo powder

CoCrMo parts are produced through selective laser meting which is based on the melting and rapid solidification of powder particles. The CoCrMo powder was produced by gas atomization under Ar and produced by LPW Technology Ltd ™. SEM imaging (Zeiss Σigma instrument, Carl Zeiss SMT Ltd ™) at 15kV shows that particles have spherical shape (Fig.1.(i)); The average particle diameter ($\bar{d}$) was measured at 33.53 µm by a granulometer

(Fig.1.(ii)). The values d(0.1) and d(0.9) are the diameters where 10% / 90% of the data is below, respectively. The chemical composition was measured through energy-dispersive X-ray (EDX) detector (EDAX™), the signal was processed and recorded by a NumeriX-DXP X10P unit, and the spectrum analysis was carried out by the software: IDFix©. The EDX system was coupled to the SEM. The values are similar to the ASTM F75 alloy as seen in Fig.1.(iii).

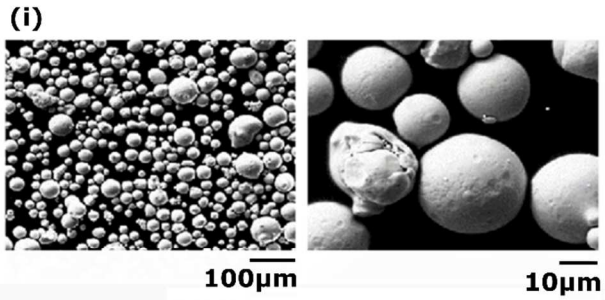

(iii)

	Co	Cr	Mo	Fe	Al	Si	Mg	W	P	S	Ni	Ti	Cu	N
Powder	Bal	28.31	6.02	0.02	0.02	0.49	0.5	<0.15	<0.01	<0.01	0.08	<0.01	Na	0.08
ASTM F75	Bal	27-30	5-7	<0.75	<0.1	<1	<1	<0.2	<0.02	<0.01	<0.5	<0.1	Na	<0.25

Figure 1 : CoCrMo Powder analysis: (i) morphology of the powder observed by SEM imaging, (ii) dry granulometry of the powder and (iii) chemical composition of the powder by EDX and comparison to the ASTM F75 standard

2.1.2 Selective laser melting

Selective laser melting (SLM) principle and the parameters used for this study are described in Fig.2. During the overall SLM process, discs are digitalised and sliced in a stack of layers (width 24µm). Each slice is developed with a scan path and adequate supports are added by the SLM software. A stripe pattern was chosen for this study, each stripe is separated by a distance of 105µm also known as the hatch vector.

Through lenses and scanning mirrors, a laser beam of 125W selectively scans and melts the powders with a specified scan path for each slice. Once a layer is finished, the building platform is lowered by an amount equal to the layer thickness, and a new layer of powders is provided from metal powder supply platform with a recoater. The process repeats until the completion of the whole part. To prevent oxidation, the process was performed under Argon gas.

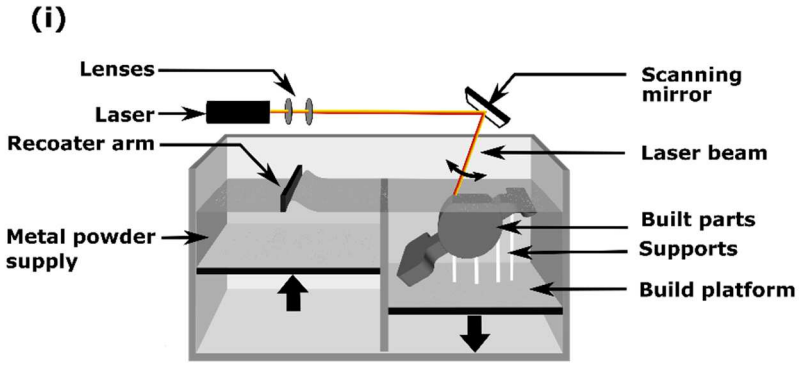

Figure 2 : Selective laser melting (SLM) process: (i) SLM principle, (ii) Manufacturing parameters strategy used

2.1.3 Superfinishing by micromachining process

Once the parts have been manufactured, surfaces usually have to be polished to achieve mirror or extremely smooth finishes to meet articular implant specifications [20]. Compared to standard-sized implants, complex and unique AM-based implant are no fitted to traditional superfinishing techniques. In an attempt to be as close as possible to the application, we used a superfinishing process that can also be applied for complex geometric parts. Specimens were superfinished by a micromachining method. It is a physico-catalyst surface treatment applied to specimens inside a liquid environment. The media used is unique and developed by the company BESTinCLASS ™ (BinC ™). The parameters of the superfinishing processes have been chosen by the industrial provider of the process directly. The advantage of the process is that it removes a uniform quantity of material and produce smooth surface mirror-like finish below 0.1µm (Ra). Our approach was to mirror-like polish our specimen using a more reproducible and automatic method [21] which might be used for complex additive manufactured implants. The test configuration is more representative of the AM-based implant reality. This is an additional element compared to literature.

Before testing, specimens were cleaned in an ultrasonic bath with, consecutively, sodium dodecyl sulfate at the critical micelle concentration 8.2 mM, acetone, ethanol, and pure water for 15min each followed by a drying of the specimens.

2.2 Multidirectional Pin-On-Disk Testing

Multidirectional pin-on-disc machine was used to perform wear tests representative of those endured by articular implant devices as seen in Fig.3. It allows to understand the general wear behavior of these materials, under the described conditions. The operating variables were chosen to mimic *in vivo* physiological and biomechanical conditions. The machine is a

custom built equipment, co-designed and assembled by RSI concept© (Lux). It allows the conduction of 3 tests simultaneously with an identicale triangular kinematics (variable point coordinates, variable speed, variable number of cycle) and the application of independent loads (variable up to 500 N). Resistances allow the heating (variable temperature) of each pin-on-disc system individualy and silicon gaiters ensure the sealing and avoids evaporation or cooling of any lubricant medium (variable volume). Therefore, this pin-on-disc machine is able to apply cross shear through several changes of direction during each cycle. In the literature, it has been demonstrated that wear on polyethylene is more relevant (and debris size and shape also) when shear forces are added to motion. More specifically, the wear rate is directly correlated to the shear rate [22,23] when nearly no mass loss is detected with unidirectional motions [24]. Indeed, the alignment of polymeric molecular chains at material surface follows the principal direction of sliding. As a consequence, multidirectional motion is necessary to generate realistic wear rates [24,25]. The standard also suggests running the test at 37 ± 2 °C to reflect body temperature. At higher test temperatures, a degradation of the protein content in the lubricant might occur creating artefacts in the results.

Physiological contact pressure was set up at 3.9MPa and applied on 7mm diameter pins taking also into account the surface states. It is representative of the contact stresses of human joints in general (between 0,5 to 5 Mpa) [26]. The lubricant was bovine serum from Biowest (Cat. S0400 - Sterile and Filtered) diluted in demineralized water with an antibiotic (Proclin 300). The total protein concentration in the mixture is 30g/L which is a clinically relevant concentration. It is filtered before use and heated at 37°C. An individual silicon gaiter ensures the sealing and avoids evaporation or cooling of the lubricant. The tests conditions were inspired by the ASTM F 732-17 Annex 2: « Wear testing of polymeric materials used in total joint prostheses », as seen in Fig.3. During the test, less than 30% of the UHMWPE pin is in contact with the diluted bovine serum and the test duration is 5 days.

(i)

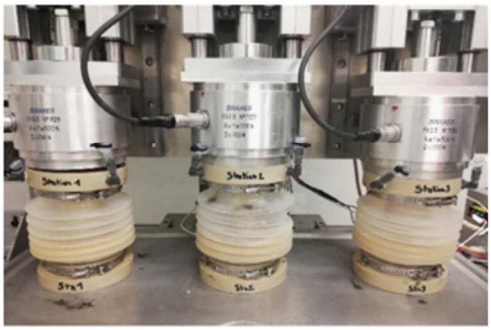

(ii)

Test protocol	Parameter
Load	150 N (i.e. 3.9 MPa)
Kinematics	Triangular (6mm for the base)
Sliding speed	Between 3035 mm/s
Number of cycles	840 000
Distance per cycle	19.4mm
Lubricant	Bovine serum (diluted at 30g/L), 37°C

Figure 3 : Pin-on-disc wear test: (i) photograph of the test running, (ii) test conditions used in this work.

2.3 Gravimetric measurements

Wear rate were analyzed by gravimetric measures. Before weighting, UHMWPE samples are rinsed with water and sodium hypochlorite (bleach), cleaned in ultrasonic bath during 10min, rinsed with water and dried with compressed air.

Gravimetric weight loss per pin was determined every 0.12, 0.24, 0.34, 0.48 and 0.84 million cycles (SARTORIUS ME 235S® with ±0.01mg of resolution and ±0.2 mg of accuracy). The weight measurements were carried out in a temperature and humidity controlled room.

2.4 Surface texture measurements

Prior to the tests, it is necessary to describe the surface texture induced by the superfinishing process, and to verify the possibility to attain Sa values in accordance with the specification of metallic bearing part of articular implant described in the standard ISO 21534: 2007.

Surface texture measurements were carried out using a confocal microscope laser (Sensofar®) on the specimens before wear testing. Roughness parameters were analyzed (SensoMAP premium® software) in order to characterize the surface of the discs at 2 different scales:

- the entire discs (assembling of zones), reflecting the geometrical deviation induce by the SLM process,
- zone of 132, 10µm x 177,44µm with an applied form removal filter (polynomial order 6). It reflects the superfinishing results of the physico-catalytic process.

Surface texture measurements were also done after the tests on the wear grooves of the CoCrMo surface and on the worn-out pins. These results were completed by SEM images (Zeiss Σigma instrument, Carl Zeiss SMT Ltd ™) and optical microscope images. The SEM accelerating voltage used was 20kV.

2.5 Microstructure and chemical composition analysis

The microstructure and chemical composition of SLM-CoCrMo parts were analyzed to have a better understanding of the material changes because of the process. To investigate the microstructure of SLM-CoCrMo, the specimens were mounted in epoxy pucks and polished up to 4000 grit paper, and finally chemical-mechanical polished with an OP-S colloidal silica solution (Struers). The microstructural-crystallographic characterization was carried out on a SEM (Zeiss Σigma instrument, Carl Zeiss SMT Ltd©) at 15kV coupled with an Electron backscatter diffraction (EBSD) system (camera: TSL-EDAX, acquisition software: Nordif, Indexation software: OIM Data collection, processing, analysis software: OIM Analysis) at 25kV. The chemical composition was measured by EDX (detector: Brucker ™, signal processing: NumeriX-DXP X10P unit, spectrum analysis software: IDFix©. 5 measurements were realized on different zones on the samples to have an average value and standard deviation.

2.6 Hardness measurements

Microstructural changes are often associated with hardness modification of the material. The hardness was measured prior the tests using a microdurometer (ZWICK ZHV-μs(H115)) in accordance to ISO-6507 and ASTM E384. The test consists of making an impact with a pyramid-shaped diamond indenter. The normal load is 300g and the residence time is 10s.

2.7 Porosity defects analysis in the sliding path

Finally, the porosity defects of the AM-CoCrMo parts were finely analyzed. Images of the cavities were taken using a digital optical microscope (Keyence®, VHX-6000) and the cavities present in the sliding path of the UHMWPE were extracted and analyzed using the integrated software (Keyence®, VHX-6000, §measure of grains). Morphology parameters including area, diameter and circularity were measured for each cavity. The circularity is described by the following equation:

$$C = \frac{\sqrt{2\pi S}}{P}$$

where C is the circularity, S the area and P the perimeter.

3 Results and discussion

3.1 Specimens Characteristics

This work focused on the tribological performance of polyethylene against superfinished SLM samples. The characteristics of the sliding surface of SLM-CoCrMo discs as well as the UHMWPE pins are detailed here.

Figure 4. (i) shows SEM micrograph taken from the superfinished sliding surface of an SLM-CoCrMo discs. The superfinished surfaces appear to be highly polished with brilliant mirror-like finished surface. The superfinishing process has also revealed pores on the surface specific to SLM materials. It indicates that the SLM samples were not fully dense. The pores have various sizes from a few microns to 1500µm. Two type of pores were revealed: (i) small and round shaped pores which are due to gas entrapment and (ii) irregular shaped pores which are the result of incomplete fusion, and/or incomplete adhesion between two successive layers, and/or a collapse of parts structure due to either a lack of support material or poor orientation. The characteristics of the pores are further described for each CoCrMo samples.

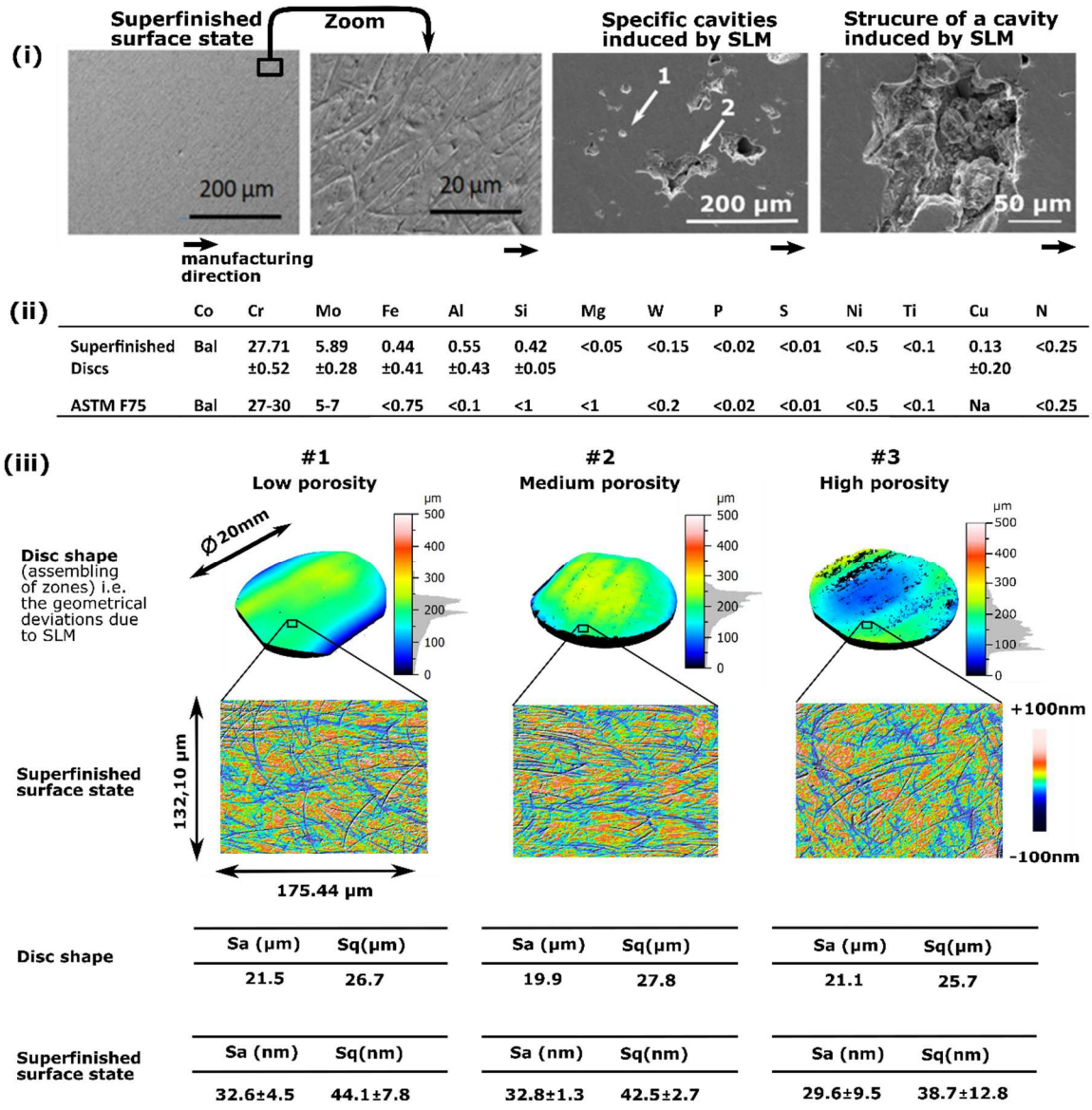

	Co	Cr	Mo	Fe	Al	Si	Mg	W	P	S	Ni	Ti	Cu	N
Superfinished Discs	Bal	27.71 ±0.52	5.89 ±0.28	0.44 ±0.41	0.55 ±0.43	0.42 ±0.05	<0.05	<0.15	<0.02	<0.01	<0.5	<0.1	0.13 ±0.20	<0.25
ASTM F75	Bal	27-30	5-7	<0.75	<0.1	<1	<1	<0.2	<0.02	<0.01	<0.5	<0.1	Na	<0.25

Figure 4 Superfinished surface: (i) SEM images showing the surface of the discs after superfinishing and the type of pores small and round pores (1) due to gas entrapment and irregular pores (2) due to sintering process, (ii) Chemical composition of the surface by EDX analysis, (iii) Surface texture measurements

The chemical composition of the superfinished surface revealed an increase in the Iron, Copper and Aluminum content compared to ASTM F75 alloy standard and the chemical composition of the CoCrMo powder (Fig.4. (ii)). It might be a contamination of the superfinishing process that was not removed by the cleaning step.

The surface is textured with submicron grooves as seen in Fig.4. (iii) with an average height roughness (Sa) of 27, 3 ±3,0nm. The obtained roughness is in the specification recommended by the ISO 21534:2007 standard: “Non-active surgical implants — Joint replacement implants — Particular requirements” which indicate a Ra maximum of 0,100nm

for the metallic part against UHMWPE, and a maximum of 50nm when the surface is convex. This surface texturation (Fig.4. (iii)) is due to the mechanical part of the superfinishing process, a flux is composed of aggregated particles of microtools created “in situ” by means of the catalyst. The average roughness parameter on the entire surfaces of all three discs was 26.5±9.4 µm (Fig.4. (iii)). It reflects the geometrical deviations that occur during the SLM process

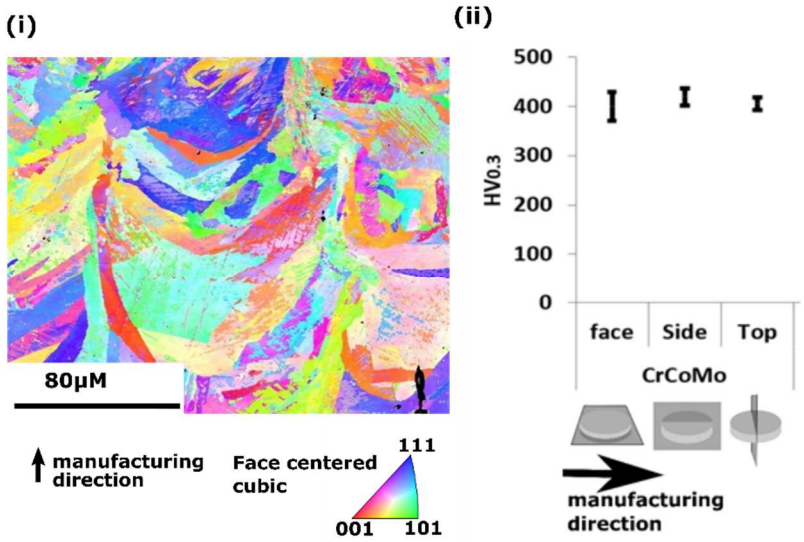

Figure 5 : (i) Microstructure revealed by EBSD analysis of the core material and (ii) impacted hardness along the different directions (HV)

SLM not only affects the surface texture but also the microstructural features of CoCrMo as shown in Fig.5.(i). The laser molten pools present an average grain size of 90µm (Fig.5.(i)) which is explained by the thermal history of the process. During SLM, materials experience fast local melting along the tracks of a high energy laser followed by rapid solidification. Due to severe temperature gradients, this material’s microstructure tends to have metastable structure [28]. The matrix is face centered cubic (fcc) (Fig.5.(i)) with precipitates at the joints of dendritic-shaped grains. No carbide was found by EDX analysis. Microstructural features changes are often impacting material properties. In our case, the resulted hardness was found to be at 400 $HV_{0,3}$ with a slight increase of 20 $HV_{0,3}$ in the direction of the building direction but not significant (Fig.5.(ii)). Comparatively, the microstructure of the cast alloy features dendrite-like structural pattern with a larger grain size [14,29]. Cast alloys also contain blocks of carbides of about 50 µm homogeneously spread into the fcc matrix. They are known to reduce the wear rate because of their very high hardness [30].

The cavities of the metallic discs located on the sliding path were fully described. Pore shape was extracted and analyzed by a set of parameters shown in fig.6.(i) and (ii)-(vii) respectively. The 3 specimens feature a gradient of porosity, 0.14%, 9,0% and 17,4% respectively for specimen #1, #2 and #3, in the sliding area as seen in fig.6.(i) and (iv). Most of the pores are small, as 75% of the pores have an area inferior to 3500μm^2 (fig.6.(ii)). These pores are due to gas entrapment during the process as seen in fig.4 (i). The analysis of the perimeter of each pore features the same tendency because of its spherical characteristics (fig.6.(iii)). The small number of large and irregular pores is the discriminating factor which leads to a difference in the ratio (%) of the overall porosity between the specimens (fig.6.(ii-iv-vi). Specimens #2 and #3 have a similar number of pores ($\approx$1500) and a similar number of pores presenting similar size distribution. The main difference results in the number of pores that are superior to 10^5 μm^2 in term of area. Specimen #1 has significantly less pores (<500). All its pores are smaller than $10^4 \mu m^2$. Analysis of the overall porosity perimeter shows a gradient between specimens which is equivalent to that of the area (fig.6.(v)).

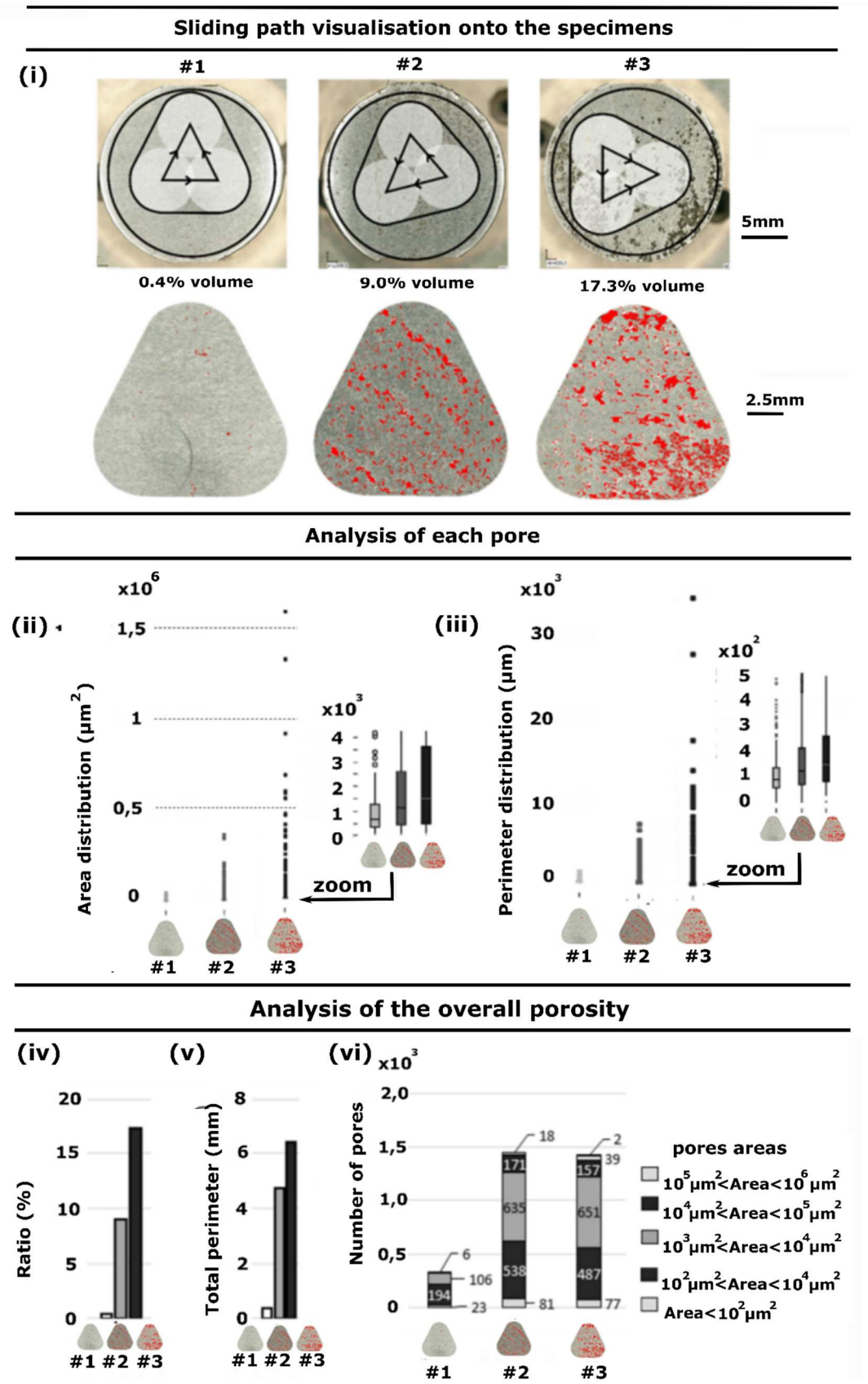

Figure 6 : Pores analysis: (i) Optical microscope images showing the path of the UHMWPE pin on the CoCrMo discs and the porosity distribution on the sliding area, (ii) area distribution of the pores, (iii) perimeter distribution of the pores, (iv) Total ratio (%) of the pores areas compared to the sliding area, (v) total perimeter and (vi) number of pores regarding the pores size.

3.2 Polyethylene Wear behavior against SLM-CoCrMo

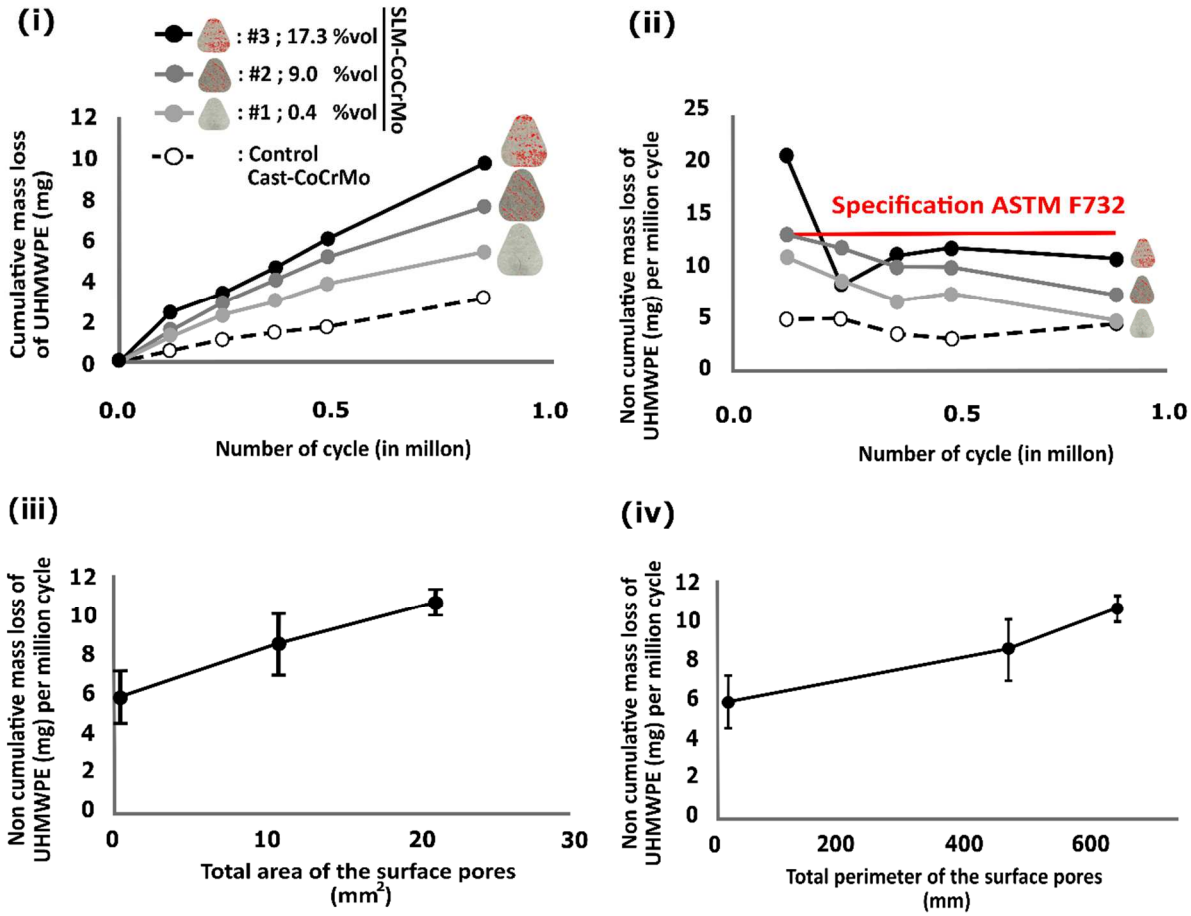

Figure 7 : Polyethylene wear against SLM-CoCrMo discs characterized by a gradient of pores: (i) cumulative mass loss of the UHMWPE pins, (ii) evolution of the non-cumulative mass loss per million cycle during the test, (iii) evolution non-cumulative mass loss results per million cycle regarding the total area of the pores, (iv) evolution of the non-cumulative mass loss results per million cycle regarding the total perimeter of the pores.

The UHMWPE mass loss results of the pins against SLM-CoCrMo discs featuring a gradient of cavities are shown in Fig.7. Throughout the test, the cumulative mass loss of the UHMWPE is higher when sliding against specimen #3 than specimen #2 followed by specimen #1. The control (cast-CoCrMo) induces the lowest wear rate. The non-cumulative mass loss per million cycle shown in Fig 7.(ii) demonstrates an initial high wear which decreases in the first 240 000 cycles. At 1 million cycle, specimen #1 (i.e. 0.4% vol porosity) has a similar wear rate than the cast version although the microstructural properties are different. Our results are within the range of wear rates reported in the litterature, which are about 7-10mg/million cycles for a standard UHMWPE [24,27]. For a cross-linked polyethylene, the wear rate is

about 2-4 mg/million cycles [25,27] where the wear rate decreases with the rise of PE crosslinking rate [22]. The mass loss values of the UHMWPE per million cycles are within the specifications recommended by the ASTM F732 standard after 240 000 cycles for all the specimens. The mass loss values of the UHMWPE per million cycles seemed linearly and positively correlated to the total area of porosity (Fig.7 (iii)) and the total perimeter of the pores (Fig.7 (iv)). Therefore, an increase of 0,213mg of polyethylene mass loss per mm^2 of pores' area is estimated. Similarly, an increase of 0,007mg of polyethylene mass loss per mm of pores' perimeter is estimated. According to Fig.7 (iii), a polyethylene mass loss of 5,5mg/million cycles is expected against a full dense SLM-CoCrMo disc. The data of Fig.7.(iv) gives an estimate of 5,1mg/million cycles. Sun *et al.* [31] performed pin-on-dics tribological test on SLM-316L against spherical stainless steel pin under dry conditions. They found that the wear rate of SLM 316L is positively correlated to the porosity percentage in terms of volume. Although the tests were performed with a different couple of materials and different tribological parameters (e.g. unlubricated condition, rotating sliding motion), the results confirm the deteriorating effect of the porosity on the wear performance of SLM parts. It is therefore essential to minimize porosity defects during the manufacturing of SLM components.

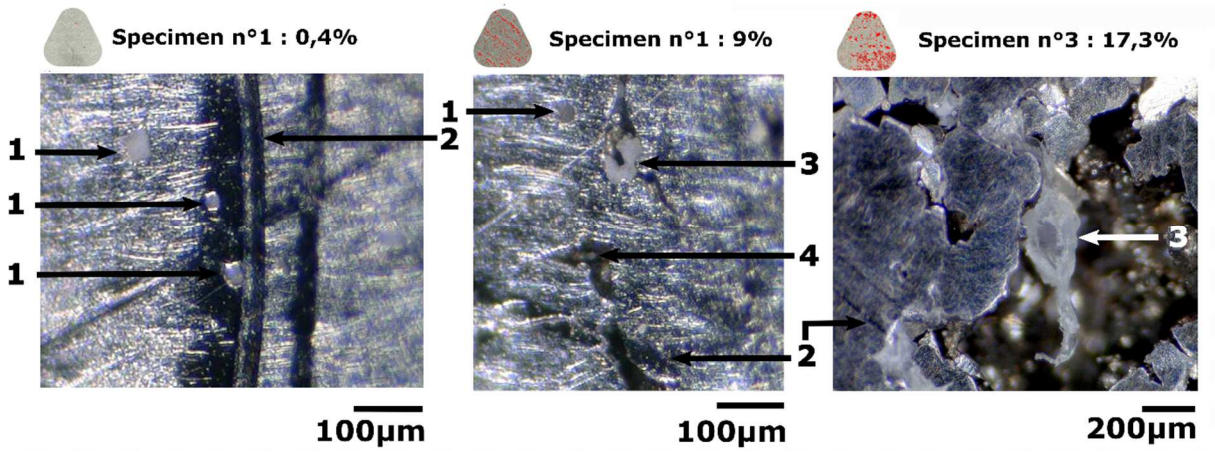

Figure 8 : UHMWPE material on the SLM-CoCrMo discs after the test; transfer of polyethylene on the metallic surface. 1 : entirelly filled pore with polyethylene; 2: trace of adhesive polyethylene; 3 : large flake-like polyethylene debris on a pore edge; 4 : round and small (10-15µm) debris of polyethylene inside a large pore; 5.

Some UHMWPE wear debris were embedded in the SLM-CoCrMo discs after the test as seen in Fig.8. In the case of specimens #1 and #2, the polyethylene debris filled the pores which are mostly small and circular. In the case of specimen #3, the polyethylene debris have also filled the small circular pores but are additionally seen at the edge of the irregular pores (Fig.8.#3). In this last configuration, the debris are much larger (Fig.8.#3) and some have a

flake shape. Specimen #2 has the same polyethylene debris type than specimen #3 but in a lower content and smaller debris size (Fig.8.#2).

All the polyethylene pins' surfaces featured triangular scratching (Fig. 9 (i)) as can be explained by the kinematics of the test. The increase in pin roughness (Sa, Sq) coincides with the increase in porosity (Fig.9 (ii) and (iii)). This confirms the abrasive behavior of the pore edge.

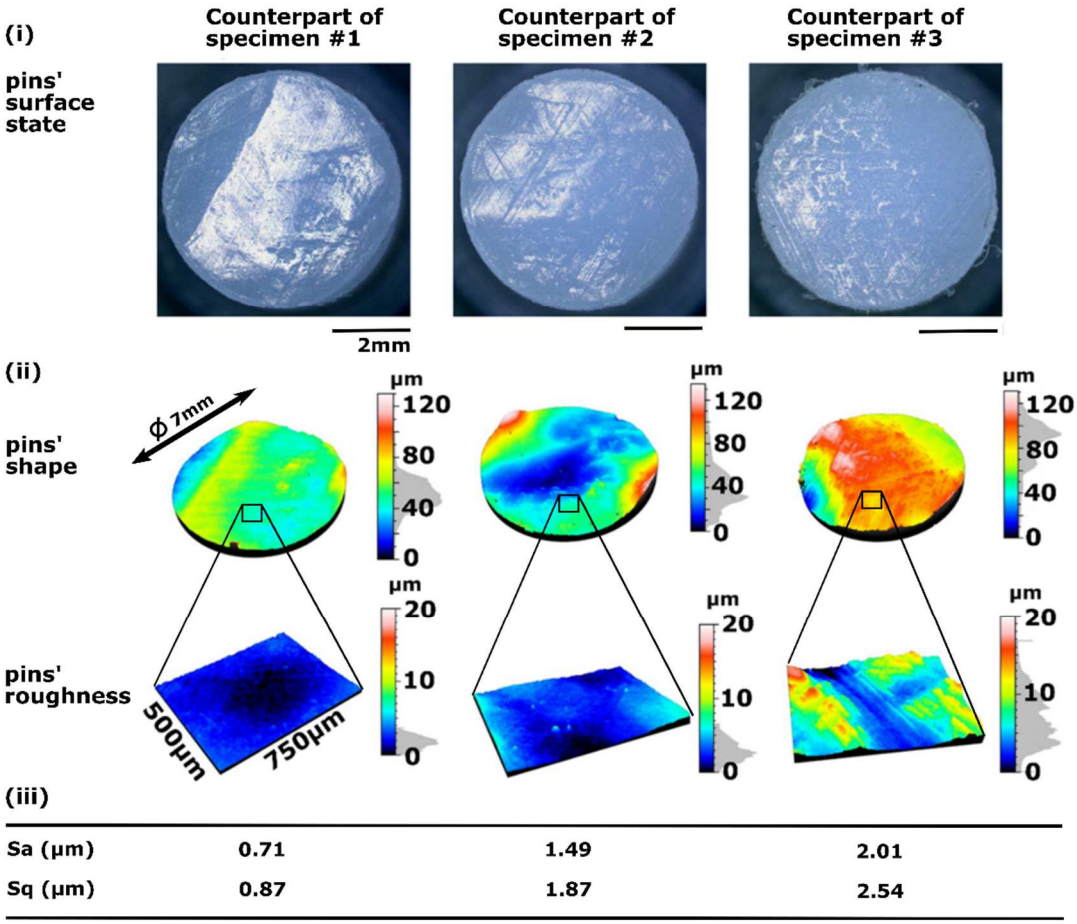

Sa (µm)	0.71	1.49	2.01
Sq (µm)	0.87	1.87	2.54

Figure 9 : Surface texturation of the UHMWPE pins after the wear test : (i) optical microscope, (ii) Non-contact 3D optical profiler of the entire surface, (iii) Non-contact 3D optical profiler of the entire surface of a zone of 500x700µm

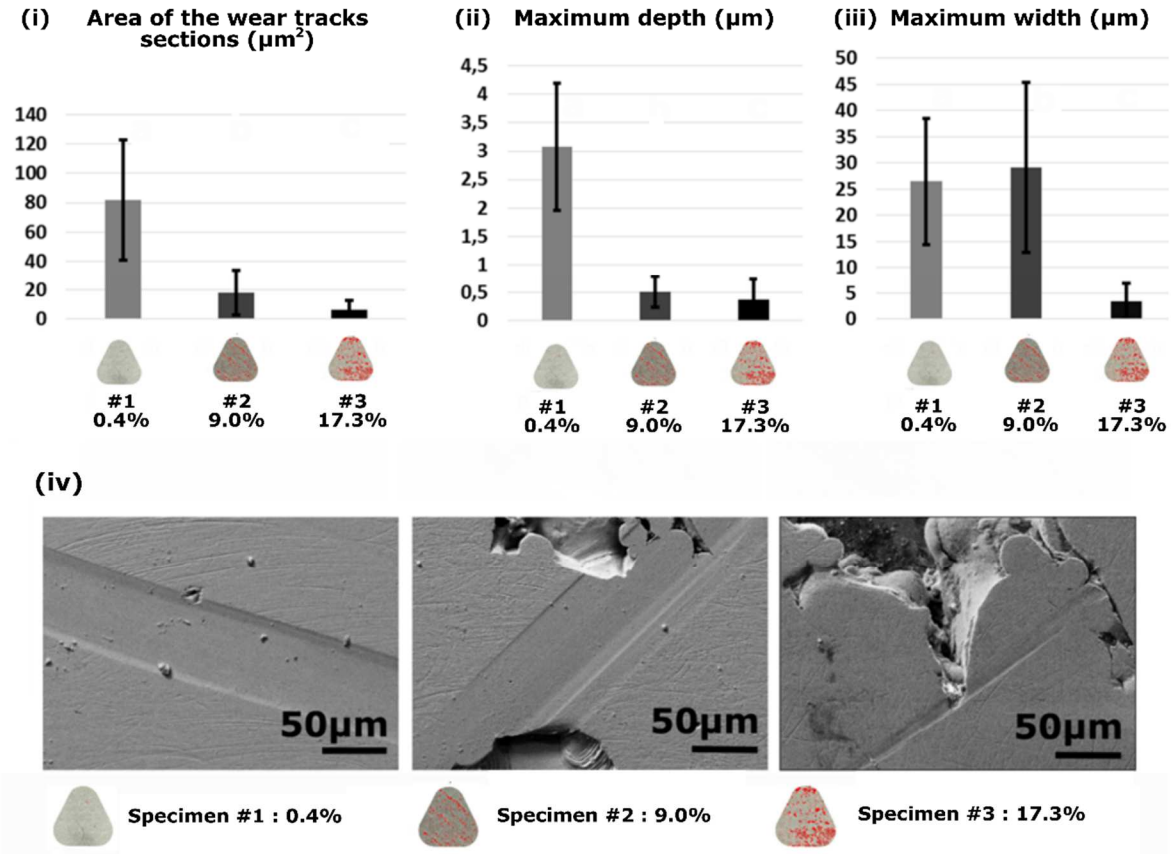

Figure 10 : Profile analysis of the wear tracks located on the CoCrMo discs after the wear test : (i) area of the wear tracks, (ii) maximum depth, (iii) maximum width and (iv) SEM images

Similarly, there were scratches visible on all the CoCrMo discs (Fig.10). Traces of burnt polyethylene were also seen at the surface of all the discs (Fig.8). Many traces are visible on the specimen #1 compared to specimens #2 and #3. These traces are typical of polymer adhesion mechanisms.

The wear tracks visible onto the surface of the disc suggest that metallic third-body particles were created during the tests. Specimen #1 had larger and deeper wear tracks compared to specimen #3. Specimen #2 had wear tracks as wide as specimen #1, but less deep. The width of the wear tracks can be explained by the morphology of the 3rd body that was formed during the test. The wear tracks of specimens #1 and #2 might reflects flat and wide debris while the wear tracks of specimen #3 might reflects small debris. The fact that specimen #3 had more irregular pores which might release metallic particles with time tends to confirm this hypothesis. The depth of the wear tracks might be explained by the potential effect of the large pores to collect debris. Indeed, these 3rd bodies tend to slide over a shorter period of time as in the presence of large pores, leading to reduced superficial wear tracks. A total absence of debris will not ever be possible. There will always be wear and tear. However, by

reducing the abrasiveness of pore edges, it would be possible to exploit their debris trapping characteristic.

Abrasion wear was therefore found on all configuration of tests resulting from two different mechanisms: (i) abrasion from the sharp pore edges on the surface and (ii) abrasion from the metallic third-body particles trapped between the surfaces.

Our work is not without limitations. Firstly, the UHMWPE samples could undergo irradiation in order to improve the wear rate [32]. Indeed, cross-linked polyethylene is mostly used for hip implants, however for other articular devices, as knee implants, it is unclear whether its superiority depends on the type of wear [33]. Because of its higher cost, production struggle and tough reticulation treatment, the standard existing polyethylene (GUR 1020) was chosen for our project. UHMWPE GUR 1050 is also used in medical joint implants; the main difference remains in its higher molecular weight (3-6 million g/mol). No statistical difference is expected between GUR 1050 and GUR 1020 in our test conditions [27].

Secondly, the results of our work show that mass loss of polyethylene is greater when the number of cavities in the AM-CoCrMo counterpart is high. However, by increasing the surface area of cavities onto the surface, the contact area decreases. It has been reported that wear factor drops with increasing contact stress [34]. Under constant load, larger contact area led to a larger wear volume.

Finally, this study was performed without soak control specimens during wear testing. Literature indicates a negligible effect since presoaking parts for 3 weeks could only induce an increase in weight between 0,2 to 0,5mg [35]. Considering that less than 30% of the UHMWPE pins are in contact with lubricant and that the test duration is 5 days in this work, the lack of soaking would likely not change general results of the performed comparative tests.

4 Conclusion

This study investigated the physical behavior of porosity defects in additive manufactured CoCrMo, by selective laser melting. A particular focus was put on the wear performance of polyethylene. It was evaluated with multidirectional pin-on-disc experiments in synovial fluid-like lubricant at 37°C. The testing conditions were set to simulate the wear of a total joint arthroplasty implant. Samples were produced by selective laser melting with

percentage of surface porosity ranging from 0.4 to 19.7%. Under the present testing conditions, all polyethylene wear rates were in accordance with the ASTM F732 standard acceptance criteria

The paper allows the following conclusions to be drawn:

- There is a strong correlation between wear rate of UHMWPE and the total area of the porosity in AM-CoCrMo discs. Reducing porosity is beneficial for improving the wear resistance of UHMWPE.
- The edges of irregular pores in SLM samples are abrasive, which leads to increased numbers if polyethylene debris and an accelerated UHMWPE mass loss during the lubricated sliding process.
- Adhesion wear was identified particularly in the nearly full-dense disc configuration. It was generated by the transfer of polyethylene material on the metallic surface.
- Abrasion wear was identified on all configuration of tests because of (i) sharp edges asperities on the surface and (ii) third -body particles trapped between the surfaces.
- The pores also limit the abrasive effect of the third body particles by acting as debris collectors.

Acknowledgements

We thank CRITT MDTS for their excellent expertise in biotribology and for the use of their cutting-edge equipment and machines.

Funding source

The work was supported by the “Agence National de la Recherche” (ANR-11-IDEX-0004-02) under Idex “Sorbonne Universités” by an IUIS project for the promotion of healthcare innovation. Augustin Lerebours was recipient of a Ph.D. fellowship from the French Ministry of Science and Technology.

Conflicts of interests

The authors have no conflicts to declare.

406 **References**

407 [1] A. Lerebours, F. Marin, S. Bouvier, C. Egles, A.C. Masquelet, A. Rassineux, A voxel-
408 based method for designing a numerical biomechanical model patient-specific with an
409 anatomical functional approach adapted to additive manufacturing, J. Numer. Sci.
410 Biomech. Bioeng. (2019).

411 [2] B. Lethaus, L. Poort, R. Böckmann, R. Smeets, R. Tolba, P. Kessler, Additive
412 manufacturing for microvascular reconstruction of the mandible in 20 patients, J.
413 Cranio-Maxillofacial Surg. 40 (2012) 43–46.

414 [3] T.R. Deshmukh, A.M. Kuthe, S.M. Chaware, B. Vaibhav, D.S. Ingole, Rapid prototyping
415 assisted fabrication of the customised temporomandibular joint implant: A case
416 report, Rapid Prototyp. J. 17 (2011) 362–368.
417 https://doi.org/10.1108/13552541111156487.

418 [4] M. Javaid, A. Haleem, Additive manufacturing applications in orthopaedics: A review,
419 J. Clin. Orthop. Trauma. 9 (2018) 202–206. https://doi.org/10.1016/j.jcot.2018.04.008.

420 [5] M.R. Hutchinson, The Burden of Musculoskeletal Diseases in the United States:
421 Prevalance, Societal and Economic Cost, 1st Edition, J. Am. Coll. Surg. 208 (2009) e5–
422 e6. https://doi.org/10.1016/j.jamcollsurg.2008.06.146.

423 [6] D. Joguet, S. Costil, H. Liao, Y. Danlos, Porosity content control of CoCrMo and
424 titanium parts by Taguchi method applied to selective laser melting process
425 parameter, Rapid Prototyp. J. 22 (2016) 20–30.

426 [7] W.E. Frazier, Metal Additive Manufacturing: A Review, J. Mater. Eng. Perform. 23
427 (2014) 1917–1928.

428 [8] H. Ali, H. Ghadbeigi, K. Mumtaz, Effect of scanning strategies on residual stress and
429 mechanical properties of Selective Laser Melted Ti6Al4V, Mater. Sci. Eng. A. 712
430 (2018) 175–187. https://doi.org/10.1016/j.msea.2017.11.103.

431 [9] S. Dadbakhsh, L. Hao, N. Sewell, Effect of selective laser melting layout on the quality
432 of stainless steel parts, Rapid Prototyp. J. 18 (2012) 241–249.

433 [10] A.E. Wilson-Heid, T.C. Novak, A.M. Beese, Characterization of the Effects of Internal

Pores on Tensile Properties of Additively Manufactured Austenitic Stainless Steel 316L, Exp. Mech. 59 (2019) 793–804. https://doi.org/10.1007/s11340-018-00465-0.

[11] P. Gokuldoss, S. Kolla, J. Eckert, Additive manufacturing processes: Selective laser melting, electron beam melting and binder jetting—Selection guidelines, Mater. . 10 (2017) 672.

[12] S. Tammas-Williams, P.J. Withers, I. Todd, P.B. Prangnell, The Effectiveness of Hot Isostatic Pressing for Closing Porosity in Titanium Parts Manufactured by Selective Electron Beam Melting, Metall. Mater. Trans. A. 47 (2016) 1939–1946.

[13] T. W., S. C., N. J., S. M., A. M. E., H. K-P., Hot Isostatic Pressing of IN718 Components Manufactured by Selective Laser Melting NRW Forschungskolleg “Leicht-Effizient-Mobil”. Energie-und kosteneffizienter Extremleichtbau mit Hybridwerkstoffen View project Twin-roll casting of aluminium-steel clad strips View project, Addit. Manuf. 13 (2017) 93–102. https://doi.org/10.1016/j.addma.2016.11.006.

[14] Y.S. Hedberg, B. Qian, Z. Shen, S. Virtanen, I. Odnevall Wallinder, In vitro biocompatibility of CoCrMo dental alloys fabricated by selective laser melting, Dent. Mater. (2014) 525–534. https://doi.org/10.1016/J.DENTAL.2014.02.008.

[15] A. Lerebours, P. Vigneron, S. Bouvier, A. Rassineux, M. Bigerelle, C. Egles, Additive manufacturing process creates local surface roughness modifications leading to variation in cell adhesion on multifaceted TiAl6V4 samples, Bioprinting. 16 (2019).

[16] I. Milošev, CoCrMo Alloy for Biomedical Applications, in: Djokić S. (Ed.), Biomed. Appl. Mod. Asp. Electrochem. Vol 55., Springer, Boston, MA, 2012. https://doi.org/10.1007/978-1-4614-3125-1_1.

[17] J.A. Disegi, R.L. Kenned, R. Pilliar, Cobalt-Base Alloys for Biomedical Applications, Danvers: A, 1999. www.copyright.comL.

[18] V.P. Mantripragada, B. Lecka-Czernik, N.A. Ebraheim, A.C. Jayasuriya, An overview of recent advances in designing orthopedic and craniofacial implants, J. Biomed. Mater. Res. Part A. (2012) 3349–3364. https://doi.org/10.1002/jbm.a.34605.

[19] ISO 5834-2: Implants for surgery — Ultra-high-molecular-weight polyethylene — Part

462 2: Moulded forms, (2019).

463 [20] ISO 21536: Non-active surgical implants – Joint replacement implants – Specific
464 requirements for knee-joint implants, (2007) 5.

465 [21] F. Bordonado, Traitement sélectif de la rugosité des surfaces. Applications
466 industrielles, Matériaux Tech. 88 (2000) 82–88.

467 [22] A. Wang, A unified theory of wear for ultra-high molecular weight polyethylene in
468 multi-directional sliding, Wear. 248 (2001) 38–47.

469 [23] E.W. Patten, D. Van Citters, M.D. Ries, L.A. Pruitt, Quantifying cross-shear under
470 translation, rolling, and rotation, and its effect on UHMWPE wear, Wear. 313 (2014)
471 125–134.

472 [24] C.R. Bragdon, D.O. O'Connor, J.D. Lowenstein, M. Jasty, S.. Biggs, W.H. Harris, A new
473 pin-on-disk wear testing method for simulating wear of polyethylene on cobalt-
474 chrome alloy in total hip arthroplasty, J. Arthroplasty. 16 (2001) 658–665.

475 [25] V. Saikko, A Hip Wear Simulator with 100 Test Stations, Proc. Inst. Mech. Eng. Part H J.
476 Eng. Med. 219 (2005) 309–318.

477 [26] R.A. Brand, Joint contact stress: a reasonable surrogate for biological processes?, Iowa
478 Orthop. J. 25 (2005) 82–94.

479 [27] S.A. Atwood, D.W. Van Citters, E.W. Patten, J. Furmanski, M.D. Ries, L.A. Pruitt,
480 Tradeoffs amongst fatigue, wear, and oxidation resistance of cross-linked ultra-high
481 molecular weight polyethylene, J. Mech. Behav. Biomed. Mater. 4 (2011) 1033–1045.

482 [28] X. Zhou, K. Li, D. Zhang, X. Liu, J. Ma, W. Liu, Z. Shen, Textures formed in a CoCrMo
483 alloy by selective laser melting, J. Alloys Compd. 631 (2015) 153–164.
484 https://doi.org/10.1016/j.jallcom.2015.01.096.

485 [29] X. Xin, J. Chen, N. Xiang, B. Wei, Surface Properties and Corrosion Behavior of Co–Cr
486 Alloy Fabricated with Selective Laser Melting Technique, Cell Biochem. Biophys. 67
487 (2013) 983–990.

488 [30] Y. Liao, E. Hoffman, M. Wimmer, A. Fischer, J. Jacobs, L. Marks, CoCrMo metal-on-
489 metal hip replacements., Phys. Chem. Chem. Phys. 15 (2013) 746–56.

[31] Y. Sun, A. Moroz, K. Alrbaey, Sliding Wear Characteristics and Corrosion Behaviour of Selective Laser Melted 316L Stainless Steel, J. Mater. Eng. Perform. 23 (2014) 518–526.

[32] V. Saikko, O. Calonius, J. Keränen, Effect of counterface roughness on the wear of conventional and crosslinked ultrahigh molecular weight polyethylene studied with a multi-directional motion pin-on-disk device, J. Biomed. Mater. Res. An Off. J. Soc. Biomater. Japanese Soc. Biomater. Aust. Soc. Biomater. Korean Soc. Biomater. 57 (2001) 506–512.

[33] B. Boyer, B. Bordini, D. Caputo, T. Neri, S. Stea, A. Toni, Is Cross-Linked Polyethylene an Improvement Over Conventional Ultra-High Molecular Weight Polyethylene in Total Knee Arthroplasty?, J. Arthroplasty. 33 (2018) 908–914. https://doi.org/10.1016/j.arth.2017.10.005.

[34] K. Vassiliou, A. Unsworth, Is the wear factor in total joint replacements dependent on the nominal contact stress in ultra-high molecular weight polyethylene contacts?, Proc. Inst. Mech. Eng. H. 218 (2004) 101–7. https://doi.org/10.1243/095441104322983997.

[35] J.Q. Yao, T.A. Blanchet, D.J. Murphy, M.P. Laurent, Effect of fluid absorption on the wear resistance of UHMWPE orthopedic bearing surfaces, Wear. 255 (2003) 1113–1120. https://doi.org/10.1016/S0043-1648(03)00167-4.